Int. J. Solids Structures, 1975, Vol. 11, pp. 887–894. Pergamon Press. Printed in Great Britain.

EFFECT OF MULTIPLE REWINDS AND TEMPERATURE CYCLES ON TIME BASE ERRORS IN VIDEO TAPE PACKS

SUBRATA MUKHERJEE†
Department of Theoretical and Applied Mechanics, Cornell University, Ithaca, NY 14850, U.S.A.

(Received 24 July 1974)

Abstract—This is a continuation of an earlier study of time base errors in video tape packs. The tape is viscoelastic. If a wound pack is stored at room temperature or subjected to multiple rewinds or environmental temperature cycles, the stresses relax and the tape creeps. Consequently, inelastic strains in the tape during playback cause distortion in the pictures. Time base error is a measure of inelastic longitudinal strain in the tape at playback. In this paper, the mathematical model developed earlier is extended to predict the effect of multiple rewinds and temperature cycles on time base error. Comparison with experiments shows very good correlation for the multiple rewind case and reasonable correlation for the temperature cycling case.

INTRODUCTION

A mathematical model was developed in [1] to predict the effect of storage time, winding pattern and pack size on time base error in video tape packs. These packs are often played back and rewound. They are also exposed to environmental temperature cycles during use. In this paper, the model from [1] is extended to include the effect of multiple rewinds and temperature cycles on time base error. Comparison with experiments is presented. We use the same notations as in [1] and often refer to equations in [1]. The assumptions given in [1] also apply here. Some further assumptions are made and these are stated later in the paper.

THE MULTIPLE REWIND MODEL

In this analysis, a rewind is assumed to mean a two pass playback plus rewind so that the location of a tape element in a pack remains unaltered after a rewind. Thus, after a certain rewind, the pack has the same stresses and elastic deformations as after any other rewind (assuming identical winding patterns in each case and an elastic hub). The difference, however, is that the tape properties are not the same in the two cases because of delayed recovery. If a piece of tape is subjected to some loading history—either creep or relaxation—and then the load is removed, the free tape, in general, recovers some part of its deformation immediately (instantaneous recovery) and some more slowly with time (delayed recovery) leaving some permanent residual deformation [2]. In our four element model (see Fig. 1, [1]) delayed recovery is due to the slow recovery of spring E_2 to its unstretched length after the load σ is removed.

The multiple rewind model has the following features: (a) Identical wind patterns are assumed at the first winding of the pack and at each successive rewind. This pattern can either be constant tension or constant torque. (b) The hub is elastic (creep parameter κ from [1] is zero). (c) At each rewind, the initial winding stresses are restored. (d) At each rewind, the inelastic radial deformations up to that time are transformed into tangential deformations. (e) At each rewind, the initial elastic radial deformations are restored. (f) Delayed recovery of the tape is included by using a method of time delayed superposition of stress and deformation histories.

Figure 1 shows a schematic outline of the model. The various stresses strains etc., used in the model are explained below.

$$n_w: \text{ Number of rewinds} + 1.$$

$$\epsilon_\theta(\bar{r}, \bar{t}) = \bar{u}(\bar{r}, \bar{t})/\bar{r}.$$

$$\bar{\sigma}_{rB}(\bar{r}, 0), \quad \bar{\sigma}_{\theta B}(\bar{r}, 0), \quad \epsilon_{\theta B}(\bar{r}, 0):$$

Beginning stresses and strains due to winding.

†This work was performed at Cartridge Television Inc., 1080 North 7th. Street, San Jose, CA 95112, U.S.A.

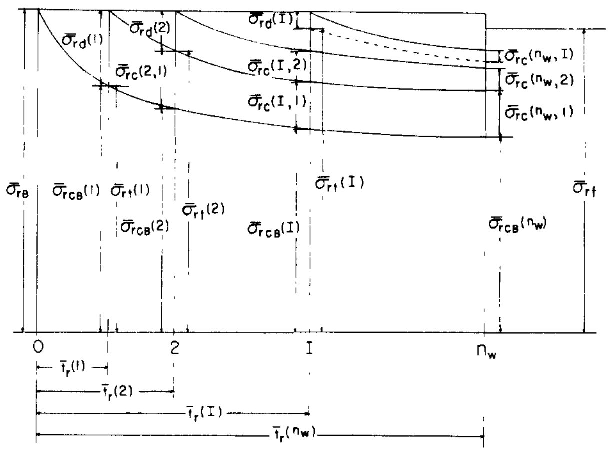

Fig. 1. Schematic diagram showing multiple rewind model.

Station (I), $I = 1, n_w$:

Stations are points in time. The tape pack is initially wound at station (0). Time is measured from here. It is played back and rewound at stations (J), $J = 1, n_w - 1$. The pack is finally unwound and time base error measured at station (n_w).

$$\bar{t}_r(I), \quad I = 1, n_w:$$

Time to station (I) from initial wind at station (0).

$$\bar{\sigma}_{rCB}(I), \quad \bar{\sigma}_{\theta CB}(I), \quad \epsilon_{\theta CB}(I), \quad I = 1, n_w:$$

Current stresses and strain at station (I) due to beginning stresses and strain $\bar{\sigma}_{rB}$, $\bar{\sigma}_{\theta B}$, $\epsilon_{\theta B}$.

$$\bar{\sigma}_{rd}(I), \quad \bar{\sigma}_{\theta d}(I), \quad \epsilon_{\theta d}(I), \quad I = 1, n_w - 1:$$

Stresses and strain added at station (I) due to rewind.

$$\bar{\sigma}_{rt}(I), \quad \bar{\sigma}_{\theta t}(I), \quad \epsilon_{\theta t}(I), \quad I = 1, n_w - 1:$$

Total stresses and strain at station (I) before $\bar{\sigma}_{rd}(I)$ etc. are added.

$$\bar{\sigma}_{rC}(M, I), \quad \bar{\sigma}_{\theta C}(M, I), \quad \epsilon_{\theta C}(M, I), \qquad M = 2, n_w; \quad I = 1, n_w - 1:$$

Interaction stresses and strain at station (M) due to added stresses and strain $\bar{\sigma}_{rd}(I)$, $\bar{\sigma}_{\theta d}(I)$, $\epsilon_{\theta d}(I)$ at station (I). Station (I) is the source station and station (M) is the effect station.

$$\bar{\sigma}_{rf}, \quad \bar{\sigma}_{\theta f}, \quad \epsilon_{\theta f}:$$

Final stresses and strain at station (n_w).

$$t_{ert}(I), I = 1, n_w - 1:$$

Radial time base error at station (I) as is measured when the tape is played back at station (I). This becomes tangential time base error at (I) when the tape is rewound.

We now present the algorithm used to calculate time base error after $n_w - 1$ rewinds. For this we must define a modified version of equation (21) of [1].

The second expression of equation (21) of [1] could be rewritten as: (see equation (28) in [1]).

$$\frac{-g_1\bar{r}}{s}(\nu_v^* - \nu_1)\bar{\sigma}_r(\bar{r}, 0) + \frac{\bar{u}(\bar{r}, 0)}{s}.$$

In the modified version of (21), the initial displacement $\bar{u}(\bar{r}, 0)$ is replaced by $\epsilon_{\theta d}(I)\bar{r}$. We call this equation (21)*.

The multiple rewind algorithm (Seee Fig. 1)
Take $\bar{r} = 1$.

Station (0). The tape pack is wound at this station. Calculate $\bar{\sigma}_{rB}$, $\bar{\sigma}_{\theta B}$, $\epsilon_{\theta B}$ from equations (26), (27) and (28) of [1].

$$\bar{\sigma}_{rB1} = \bar{\sigma}_{rB} \quad \text{at} \quad \bar{r} = 1.$$

Calculate $\bar{\sigma}_{rCB}$ etc. at all subsequent stations 1, n_w. For $J = 1$, n_w:

$$\left.\begin{array}{l} \bar{\sigma}_{rB} \\ \bar{\sigma}_{rB1} \\ \bar{\sigma}_{\theta B} \\ \bar{t} = \bar{t}_r(J) \end{array}\right\} \Rightarrow \begin{array}{c} \text{Equations} \\ (21), (22), (23) \\ \text{of [1]} \end{array} \Rightarrow \begin{array}{l} \bar{\sigma}_{rCB}(J) \\ \bar{\sigma}_{\theta CB}(J) \\ \epsilon_{\theta CB}(J). \end{array}$$

Station (1). The tape pack is played back and rewound here for the first time. Calculate $\bar{\sigma}_{rd}$, $\bar{\sigma}_{rt}$, t_{ert} etc. at station (1).

$$\bar{\sigma}_{rd}(1) = \bar{\sigma}_{rB} - \bar{\sigma}_{rCB}(1).$$

Similarly for $\bar{\sigma}_{\theta t}(1)$, $\epsilon_{\theta t}(1)$.

$$\bar{\sigma}_{rd1}(1) = \bar{\sigma}_{rd}(1) \quad \text{at} \quad \bar{r} = 1.$$

$$\bar{\sigma}_{rt}(1) = \bar{\sigma}_{rB} - \bar{\sigma}_{rd}(1).$$

Similarly for $\bar{\sigma}_{\theta t}(1)$, $\epsilon_{\theta t}(1)$.

$$t_{ert}(1) = \{\epsilon_{\theta t}(1) + g_1(\nu_1 - \gamma)\bar{\sigma}_{rt}(1)\}/k.$$

Calculate interaction stresses $\bar{\sigma}_{rC}$ etc. at all subsequent stations 2, n_w due to $\bar{\sigma}_{rd}$ etc. at station (1).
For $J = 1$, $n_w - 1$; $n_w > 1$:

$$\left.\begin{array}{l} \bar{\sigma}_{rd}(1) \\ \bar{\sigma}_{rd1}(1) \\ \bar{\sigma}_{\theta d}(1) \\ \epsilon_{\theta d}(1) \\ \bar{t} = \bar{t}_r(1+J) - \bar{t}_r(1) \end{array}\right\} \Rightarrow \begin{array}{c} \text{Equations (21)*} \\ \text{and (22), (23)} \\ \text{of [1]} \end{array} \Rightarrow \begin{array}{l} \bar{\sigma}_{rC}(1+J, 1) \\ \bar{\sigma}_{\theta C}(1+J, 1) \\ \epsilon_{\theta C}(1+J, 1). \end{array}$$

Station (*I*). $I = 2$, $n_w - 1$; $n_w > 2$:
Calculate $\bar{\sigma}_{rd}$, $\bar{\sigma}_{rt}$, t_{ert} etc. at station (I).

$$\bar{\sigma}_{rd}(I) = \bar{\sigma}_{rB} - \bar{\sigma}_{rCB}(I) - \sum_{M=1}^{I-1} \bar{\sigma}_{rC}(I, M).$$

Similarly for $\bar{\sigma}_{\theta d}(I)$, $\epsilon_{\theta d}(I)$.

$$\bar{\sigma}_{rd1}(I) = \bar{\sigma}_{rd}(I) \quad \text{at} \quad \bar{r} = 1.$$

$$\bar{\sigma}_{rt}(I) = \bar{\sigma}_{rB} - \bar{\sigma}_{rd}(I).$$

Similarly for $\bar{\sigma}_{\theta t}(I)$, $\epsilon_{\theta t}(I)$.

$$t_{ert}(I) = [\epsilon_{\theta t}(I) + g_1(\nu_1 - \gamma)\bar{\sigma}_{rt}(I)]/k.$$

Calculate $\bar{\sigma}_{rC}$ etc. at all subsequent stations $I+1$, n_w due to $\bar{\sigma}_{rd}$ etc. at station (I). For $J = 1$, $n_w - I$:

$$\left.\begin{array}{l}\bar{\sigma}_{rd}(I)\\ \bar{\sigma}_{rd1}(I)\\ \bar{\sigma}_{\theta d}(I)\\ \epsilon_{\theta d}(I)\\ \bar{t} = \bar{t}_r(I+J) - \bar{t}_r(I)\end{array}\right\} \Rightarrow \begin{array}{l}\text{Equations (21)*}\\ \text{and (22), (23)}\\ \text{of [1]}\end{array} \Rightarrow \begin{array}{l}\bar{\sigma}_{rC}(I+J, I)\\ \bar{\sigma}_{\theta C}(I+J, I)\\ \epsilon_{\theta C}(I+J, I).\end{array}$$

Station (n_w). The pack is finally unwound and time base error is measured here. Calculate $\bar{\sigma}_{rf}$ etc. and time base error. If $n_w = 1$, $\bar{\sigma}_{rf} = \bar{\sigma}_{rCB}(n_w)$. If $n_w > 1$,

$$\bar{\sigma}_{rf} = \bar{\sigma}_{rCB}(n_w) + \sum_{M=1}^{n_w - 1} \bar{\sigma}_{rC}(n_w, M).$$

Similarly for $\bar{\sigma}_{\theta f}$, $\epsilon_{\theta f}$.

$$t_{er} = [\epsilon_{\theta f} + g_1(\nu_1 - \gamma)\bar{\sigma}_{rf}]/k.$$

If $n_w = 1$, $t_{et} = [\bar{\sigma}_{\theta B} - \bar{\sigma}_{\theta CB}(n_w)]g_1/k$. If $n_w > 1$,

$$t_{et} = \left\{\bar{\sigma}_{\theta B} - \bar{\sigma}_{\theta CB}(n_w) + \sum_{I=1}^{n_w-1} \bar{\sigma}_{\theta d}(I) - \bar{\sigma}_{\theta C}(n_w, I)\right\} g_1/k + \sum_{I=1}^{n_w-1} t_{ert}(I).$$

$$t_e = t_{er} + t_{et}.$$

Repeat for other values of $\bar{r}$ till $\bar{r} = R$. This gives us the time base error distribution in the tape pack after $n_w - 1$ rewinds.

THE TEMPERATURE CYCLING MODEL

This analysis is an extension of Tramposch[3]. As in [3], a temperature cycle means the following: a tape pack, immediately after completing the winding, is stored at a higher but constant temperature. After storage for some time, the pack is cooled to the winding temperature and the time base error measured immediately. The heating and cooling processes are assumed instantaneous, i.e. thermal transients are neglected.

Tramposch [3] included the effect of thermal stresses due to the hub having a larger coefficient of thermal expansion than the tape. This is included here but the model is formulated somewhat differently. In addition, we include a viscoelastic hub (as in [1]) and allow for change of properties of the hub and tape materials with temperature.

The thermal stresses and displacement are calculated by solving an axisymmetric problem of a thin viscoelastic disc in plane stress[4]. The disc has inside and outside radii 'a' and 'b' respectively and is supported by a viscoelastic hub of outside radius 'a'. The hub has a larger coefficient of thermal expansion than the tape (see Fig. 1 in [1]).

The boundary conditions are:

$$\bar{r} = R: \quad \bar{\sigma}^*_{rth} = 0,$$

$$\bar{r} = 1: \quad \bar{u}^*_{th} = g_1 F^*_v \bar{\sigma}_{rth} + \frac{T\alpha w}{s}, \tag{1}$$

where

$$\sigma_{rth}, \quad \sigma_{\theta th}, \quad u_{th}$$

are the thermal stresses and displacement. As in [1], $^-$ denotes a nondimensionalized quantity and * the Laplace transform.

$$T_{\alpha w} = (\alpha_h - \alpha_t)(T - T_w),$$

where

α_h, α_t: are the coefficients of linear thermal expansion of the hub and tape respectively.
T_w: is the winding temperature.
T: is the elevated temperature to which the tape pack is heated.

The solution is given by:

$$\bar{u}^*_{th}(\bar{r}, s) = \frac{T\alpha w[(1-\nu^*_v)\bar{r} + (1+\nu^*_v)R^2/\bar{r}]}{s[(g_1F^*_v\bar{E}^*_v + \nu^*_v)(R^2-1) + (R^2+1)]} \tag{2}$$

$$\bar{\sigma}^*_{rth}(\bar{r}, s) = \frac{T\alpha w\bar{E}^*_v(1 - R^2/\bar{r}^2)}{s[(g_1F^*_v\bar{E}^*_v + \nu^*_v)(R^2-1) + (R^2+1)]} \tag{3}$$

$$\bar{\sigma}^*_{\theta th}(\bar{r}, s) = \frac{T\alpha w\bar{E}^*_v(1 + R^2/\bar{r}^2)}{s[(g_1F^*_v\bar{E}^*_v + \nu^*_v)(R^2-1) + (R^2+1)]}. \tag{4}$$

These transforms can be easily inverted once the values of $\bar{E}^*_v$, ν^*_v and F^*_v are substituted from equations (3), (4) and (8) of [1]. The values of g_1, g_2, g_3, ν_1, F and κ at the elevated temperature T must be used.

The radial stress in the wound pack after storage for time $\bar{t}$ at the elevated temperature T is given by the sum of the stresses due to winding and due to heating

$$\bar{\sigma}_{rtw}(\bar{r}, \bar{t}) = \bar{\sigma}_r(\bar{r}, \bar{t}) + \bar{\sigma}_{rth}(\bar{r}, \bar{t}), \tag{5}$$

and similarly for $\bar{\sigma}_{\theta tw}(\bar{r}, \bar{t})$ and $\epsilon_{\theta tw}(\bar{r}, \bar{t})$. (Note $\epsilon_\theta = \bar{u}/\bar{r}$).

$\bar{\sigma}_r(\bar{r}, \bar{t})$ etc. are obtained from equations (21), (22) and (23) of [1].

Cooling means removal of the initial thermal stresses. Thus, after a temperature cycle during which the pack was stored for time $\bar{t}$ at temperature T, we get the final value of the radial stress in the wound pack.

$$\bar{\sigma}_{rfn}(\bar{r}, \bar{t}) = \bar{\sigma}_r(\bar{r}, \bar{t}) + \bar{\sigma}_{rth}(\bar{r}, \bar{t}) - \bar{\sigma}_{rth}(\bar{r}, 0), \tag{6}$$

and similarly for $\bar{\sigma}_{\theta fn}$, $\epsilon_{\theta fn}$.

Unwinding is simulated as in Table 1 [1]. The time base error therefore is:

$$t_e = [\epsilon_{\theta fn}(\bar{r}, \bar{t}) + g_1(\nu_1 - \gamma)\bar{\sigma}_{rfn}(\bar{r}, \bar{t})]/k + [\bar{\sigma}_\theta(\bar{r}, 0) - \bar{\sigma}_{\theta fn}(\bar{r}, \bar{t})]g_1/k. \tag{7}$$

Note that in equation (7) material properties at the winding temperature T_w must be used.

RESULTS AND CONCLUSIONS

Numerical calculations have been carried out for the following values of the parameters using a digital computer, assuming constant torque winding for some cases and constant tension winding for others:

Tape Material Properties
At the winding temperature $T_w = 70°F$ (21·1°C):

$E_1 = 0{\cdot}5 \times 10^6$ psi ($0{\cdot}345 \times 10^5$ bar), $E_2 = 0{\cdot}2 \times 10^7$ psi ($0{\cdot}138 \times 10^6$ bar),

$E_3 = 0{\cdot}5334 \times 10^8$ psi ($0{\cdot}368 \times 10^7$ bar), $\nu_1 = 0{\cdot}35$,

$\tau_2 = 2$ days, $\alpha_t = 0{\cdot}944 \times 10^{-5}$/°F ($1{\cdot}70 \times 10^{-5}$/°C).

At the elevated temperature $T = 113°F$ (45°C):

$E_1 = 0{\cdot}35 \times 10^6$ psi ($0{\cdot}242 \times 10^5$ bar), $E_2 = 0{\cdot}2 \times 10^7$ psi ($0{\cdot}138 \times 10^6$ bar),

$E_3 = 0{\cdot}5334 \times 10^8$ psi ($0{\cdot}368 \times 10^7$ bar), $\nu_1 = 0{\cdot}35$,

$\tau_2 = 12$ hours, $\alpha_t = 0{\cdot}944 \times 10^{-5}$/°F ($1{\cdot}70 \times 10^{-5}$/°C).

Other Parameters:

$$a = 1{\cdot}25\ \text{in}\ (3{\cdot}18\ \text{cm}).$$

Tape width = 0·5 in (1·27 cm). Tape thickness = $0{\cdot}97 \times 10^{-3}$ in ($0{\cdot}246 \times 10^{-2}$ cm).

$$k = 6 \times 10^{-5}/\mu\,\text{sec}.$$

$$\alpha_h = 0{\cdot}39 \times 10^{-4}/°\text{F}\ (0{\cdot}7 \times 10^{-4}/°\text{C})\ \text{for polystyrene hub}.$$

$$\alpha_h = 0{\cdot}129 \times 10^{-4}/°\text{F}\ (0{\cdot}232 \times 10^{-4}/°\text{C})\ \text{for aluminium hub}.$$

Subsequent figures show the computed results for a number of appropriate values of the hub flexibility and creep parameter F and κ and pack diameter ratio R.

Figure 2 shows a comparison of time base error predicted by the rewind model with experimental observations for a 4 in (10·16 cm) diameter pack subjected to multiple rewind histories as shown. The hub is made of polystyrene (viscoelastic) and is nonuniform, but is modelled as elastic with an average flexibility $F = 3{\cdot}0$. Neglecting hub creep does not make too much difference at room temperature but causes large errors at elevated temperatures. As in [1], time base error was measured electronically using a cross-field television monitor.

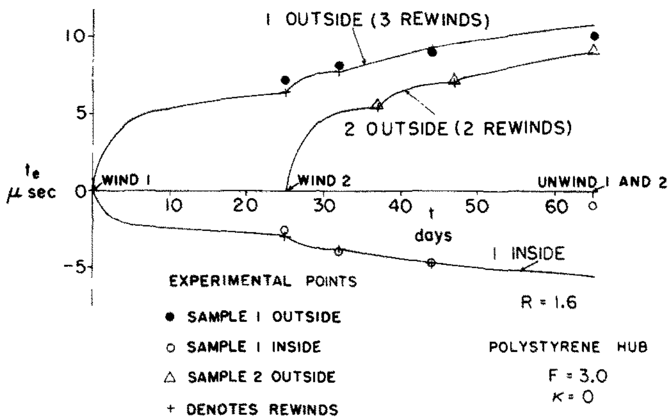

Fig. 2. Effect of multiple rewinds on time base error. Constant tension winding at 5 oz (1·39 N) at first wind and at each successive rewind.

The correlation is excellent except for the last point in the inside of sample 1. As expected, the time base error grows fast with time initially, but the rate of increase decreases with time. At the first rewind point there is a marked increase in slope as the time base error increases faster than it would without the rewind. Subsequent rewinds have progressively less effect. In both samples, the time base error on the outside tends to nearly equal values.

The effect of rewinds on time base error is further illustrated in Fig. 3. Rewinds equally

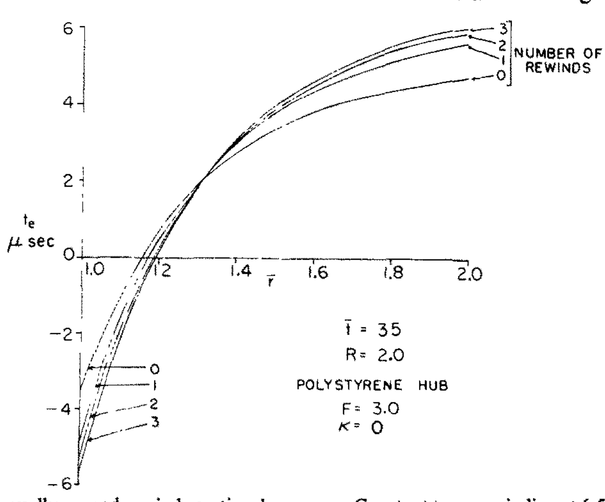

Fig. 3. Effect of equally spaced rewinds on time base error. Constant torque winding at 6·5 in-oz (0·046 N.m) at first wind and at each successive rewind.

spaced in time at the same torque level on a 5 in (12·7 cm) diameter pack are considered. In each case the storage time $\bar{t} = 35$ and the time base error is measured at the end of this period. Sample 0 is stored undisturbed, sample 1 is played back and rewound once after $\bar{t} = 17{\cdot}5$, sample 2 is played back and rewound twice after $\bar{t} = 35/3$ and 70/3 etc. Rewinds increase absolute values of time base error in packs. Note, however, that this effect is progressively less as the number of rewinds within the same time span increases and for 3 rewinds the time base error is already approaching an asymptotic distribution. Physically, an asymptotic distribution amounts to new rewinds at every instant so that stresses are never allowed to relax Creep, of course, takes place.

The rewind model can be used to study the effect of initial (pre-recording) stress-deformation history in the tape on time base error. It can also be used to determine if the tape can be subjected to a certain stress-deformation pre-history (before recording on it) so that this will partially compensate for time base errors during pack storage. This would mean using recovery to compensate for creep and relaxation.

Figure 4 shows time base error due to temperature cycling for various pack sizes. $\bar{\delta}$ is the calculated value of reduction of hub diameter after temperature cycling due to hub creep.

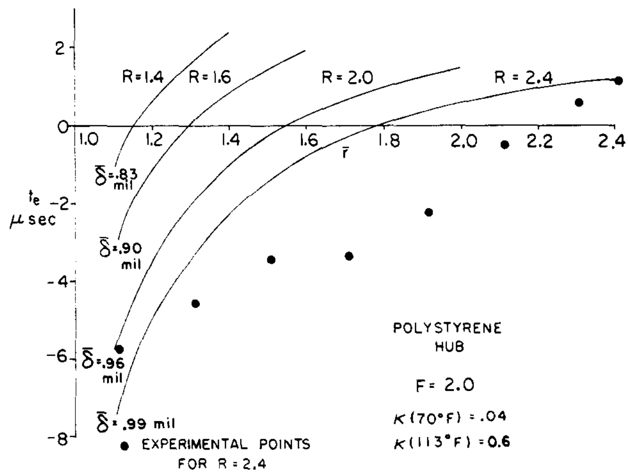

Fig. 4. Time base error due to temperature cycling for various pack sizes. Constant torque winding at 6·25 in-oz (0·044 N.m). $T_w = 70°F$ (21·1°C). Stored at 113°F (45°C) for 16 hr. Polystyrene hub. 1 mil = 0·0025 cm.

As in Fig. 4[1], the smaller the pack, the larger the outside winding tension (for constant torque winding) and the lower the hub pressure. Thus, with decreasing pack size, the absolute value of time base error increases at the outside and decreases near the hub. The time base error at the hub is due not only to hub creep but radial and tangential relaxation as well. This is seen from the fact that the absolute value of time base error near the hub decreases far more rapidly with decreasing pack size than does hub creep. Creep of the hub causes fairly large compressive hoop stresses in the tape near it. In the 6 in (15·24 cm) diameter pack ($R = 2{\cdot}4$) the compressive hoop stress in a tape layer near the hub due to winding becomes more compressive after storage at 113°F (45°C) for 16 hours. Sufficiently long storage at 113°F (45°C) would, of course, cause the hoop stress to relax to zero.

The theoretical curve for $R = 2{\cdot}4$ is compared with an experiment. The minimum and maximum values agree quite well but the theoretical curve rises much more steeply near the hub and tapers off near the outside. The value at the outside is positive both from theory and experiment while measurements showed some decrease of outside diameter of the pack after temperature cycling. This is explained by the fact that although radial creep is negative at the outside (this is seen from the theory as well) the time base error is positive because of the positive contribution of tangential relaxation. The positive tension outside relaxes without any tangential motion of the tape, thus causing positive time base error.

The discrepancy between theory and experiment is primarily due to lack of knowledge of creep properties of the hub and the tape at elevated temperatures. The properties used here matched the measured decrease of hub diameter of one mil (0·0025 cm) for the 6 in (15·24 cm) diameter pack. The tape properties used in the calculations would cause the tape to creep 0·0138 per cent in three hours at 1200 psi (82·74 bar) and 113°F (45°C). This agrees reasonably well with experimental data from other investigators working with high polymers. Use of carefully measured creep properties should improve correlation with the experiment. Another unknown is the behavior of the magnetic coating at elevated temperatures. In this model the coating was assumed to creep like mylar. Also, pre-recording stress-deformation history of the tape was ignored.

Figure 5 shows results of calculations using data for an uniform aluminium hub. The stiffer elastic hub greatly reduces absolute values of time base error due to temperature cycling and the distribution becomes nearly uniform across the pack.

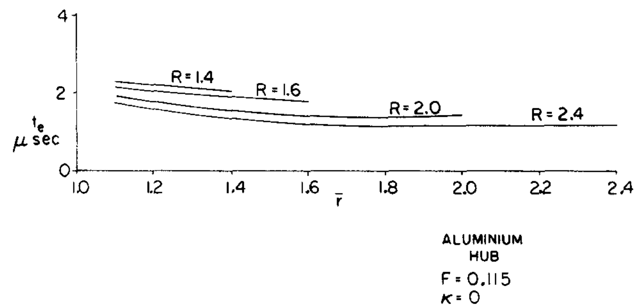

Fig. 5. Time base error due to temperature cycling for various pack sizes. Constant torque winding at 6·25 in-oz (0·044 N.m). T_w = 70°F (21·1°C). Stored at 113°F (45°C) for 16 hr. Aluminium hub.

This paper, together with [1], has tried to predict the effect of several engineering variables of interest on time base error in video tape packs. Further research is necessary to determine optimum hub and tape properties, winding patterns and stress-deformation pre-histories with a view to minimizing time base error. Proper understanding of the mechanics should make it simpler and cheaper to correct time base error electronically during playback.

This analysis for video tape packs applies equally well to audio and digital tapes. If information tracks are nearly perpendicular to the tape edge lateral strains are of interest and the model must be suitably extended using Poisson's ratio of the tape.

Acknowledgements—Sincere thanks are expressed to Cartridge Television for making this work possible, to Mr. Philip Smaller for his invaluable suggestions throughout the course of this investigation and for his performing of the experiments and to Mr. Vladimir Lieskovsky for various useful comments.

REFERENCES

1. S. Mukherjee, Time base errors in video tape packs. *J. Appl. Mech.* **41**, (3), *Trans. ASME*, Vol. 96, Series E, pp. 625–630 (Sept. 1974).
2. H. Tramposch, Relaxation of internal forces in a wound reel of magnetic tape. *J. Appl. Mech.* **32**, (4), *Trans. ASME*, Vol. 87, Series E, pp. 865–873 (Dec. 1965).
3. H. Tramposch, Anisotropic relaxation of internal forces in a wound reel of magnetic tape. *J. Appl. Mech.* **34**, (4), *Trans. ASME*, Vol. 89, Series E, pp. 888–894 (Dec. 1967).
4. S. P. Timoshenko, Two dimensional problems in polar coordinates. *Theory of Elasticity*, 3rd edition. pp. 65–149. McGraw-Hill, New York (1970).